Statistical characteristics of radio source scintillations at decameter wavelengths

M.M. Kalinichenko[1,2], N.V. Kuhai[2,1], O.O. Konovalenko[1],
O.I. Romanchuk[1], A.I. Brazhenko[3] ,
O.L. Ivantishin[4], T.A. Stasiuk[5]

[1] Institute of Radio Astronomy of NASU, Ukraine;

[2] Oleksandr Dovzhenko Hlukhiv National Pedagogical University, Ukraine ,

[3] Gravimetrical observatory of Geophysical institute of NASU, Ukraine

[4] Institute of physics and mechanics of NASU, Lviv, Ukraine;

Ukrainian low frequency radio telescopes on the map of Europe

Figure 1

Outward appearance of Ukrainian low frequency radio telescopes

UTR-2, 8 – 32 MHz (Kharkiv)

URAN-2, 8 – 32 MHz (Poltava)

URAN-4, 8 – 32 MHz (Odesa)

URAN- 1, 8 – 32 MHz (Zmiev)

URAN- 3, 8 – 32 MHz (Lviv)

GURT, 8 – 80 MHz (Kharkiv)

Figure 2

Investigations of the interplanetary scintillations (IPS)

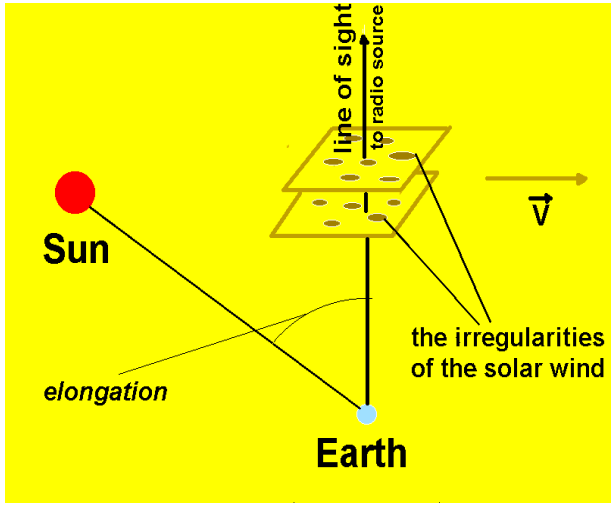

Fig. 3. Interplanetary scintillations (IPS)

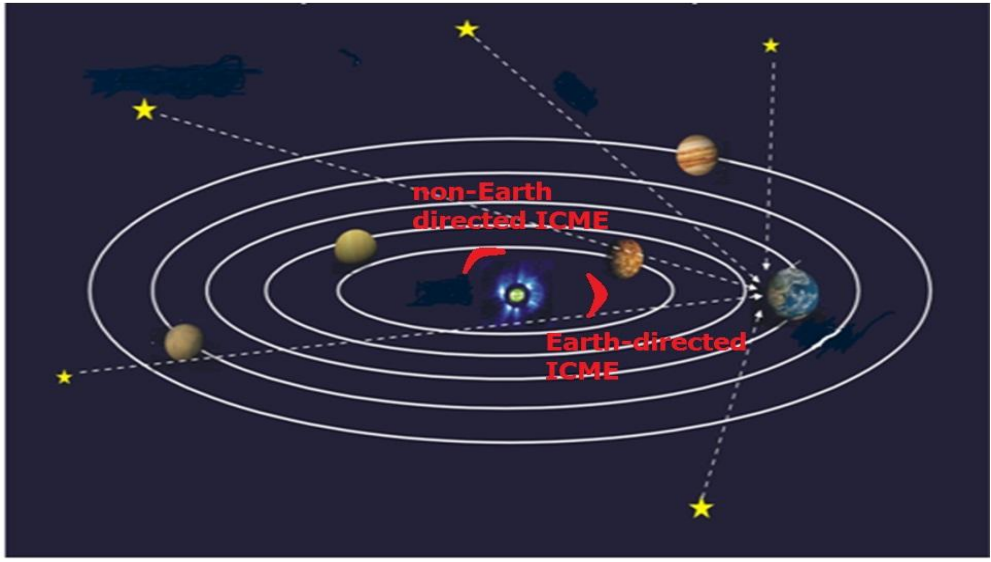

Fig. 4. Whole heliosphere monitoring
with using Ukrainian radio telescopes

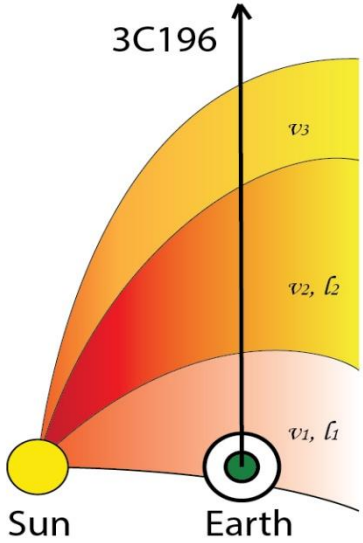

Fig. 5. Founding and tracking of geoeffective ICMEs and CIRs by using IPS data from Ukrainian radio telescopes

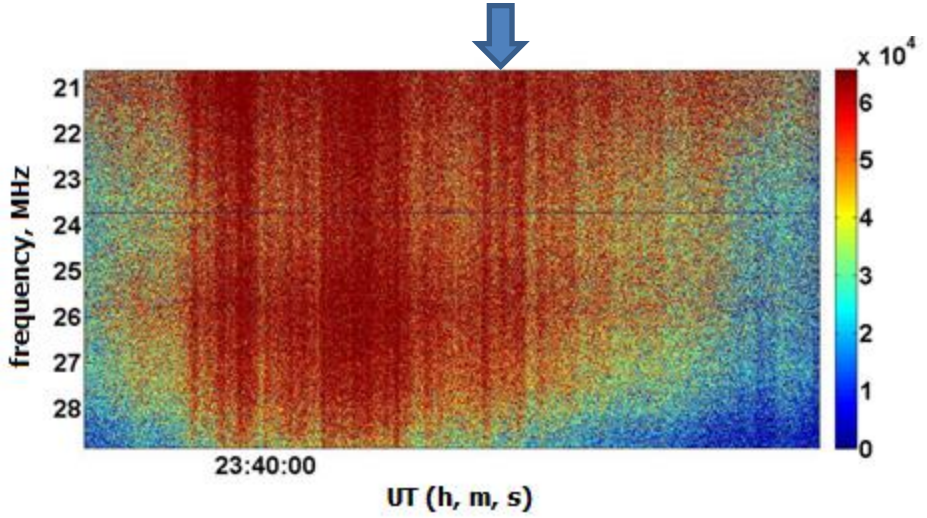

Fig. 6. An example of registration of interplanetary scintillations. UTR-2 radio telescope.

Experimental IPS data processing

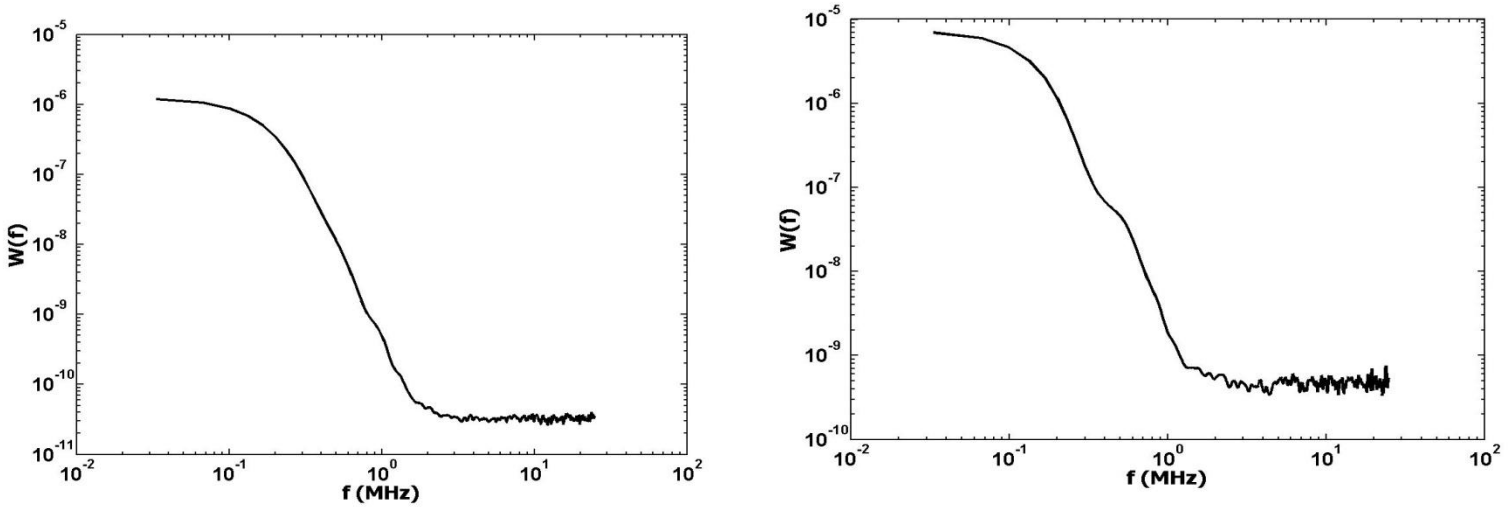

Fig.7. Experimental spectra for one (left) and two (right) stream cases.

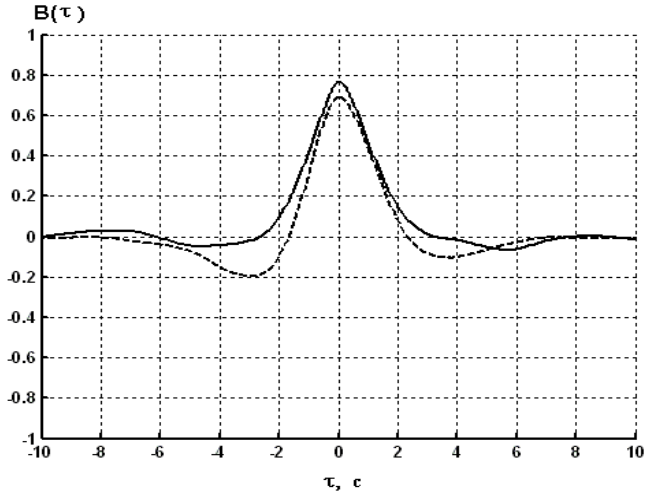

Fig.8. Experimental cross-correlation function for one (solid line) and two (dashed line) stream cases

Model fitting

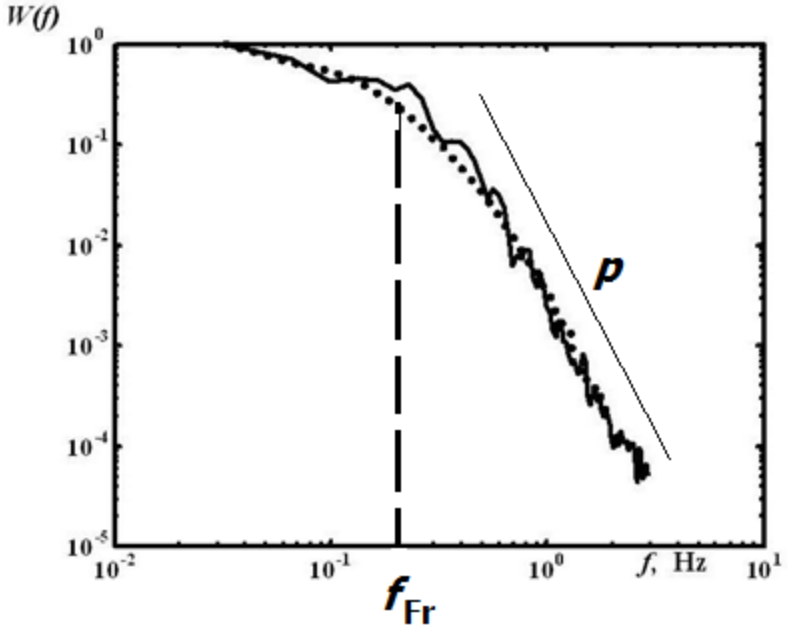

Figure 9. Scintillation spectrum

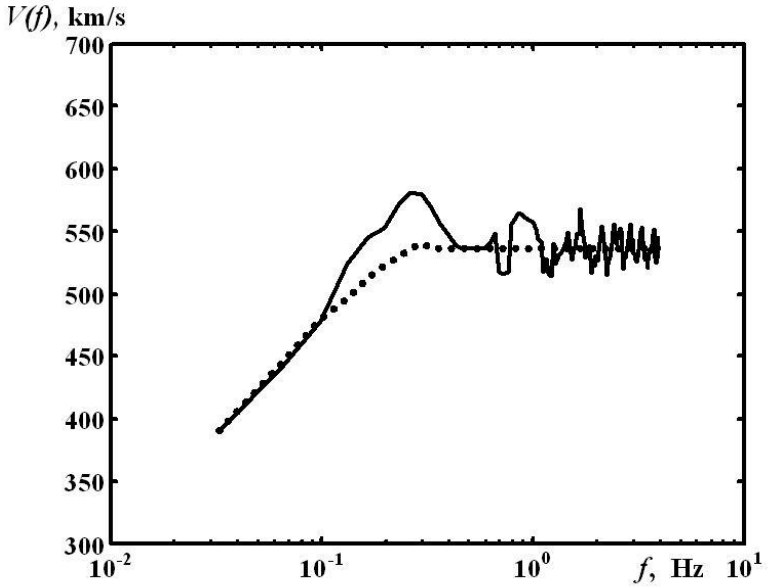

Fig. 10. Velocity of cross spectrum harmonics

$$V_f(f) = 2\pi f b \cos\beta / \Delta\Psi$$

Here $\Delta\Psi = \arccos\left(\mathrm{Re}W(b, f)/|W(b, f)|\right)$

is the phase shift between the antennas for f

-harmonic of cross spectrum $W(b, f)$

Observations

We have carried out regular IPS observations of a set of radio sources including the most powerful radio sources at decameter radio waves in the sky: Virgo A (3C274), Cassiopeia A (3C461) and Crab nebula (3C144)

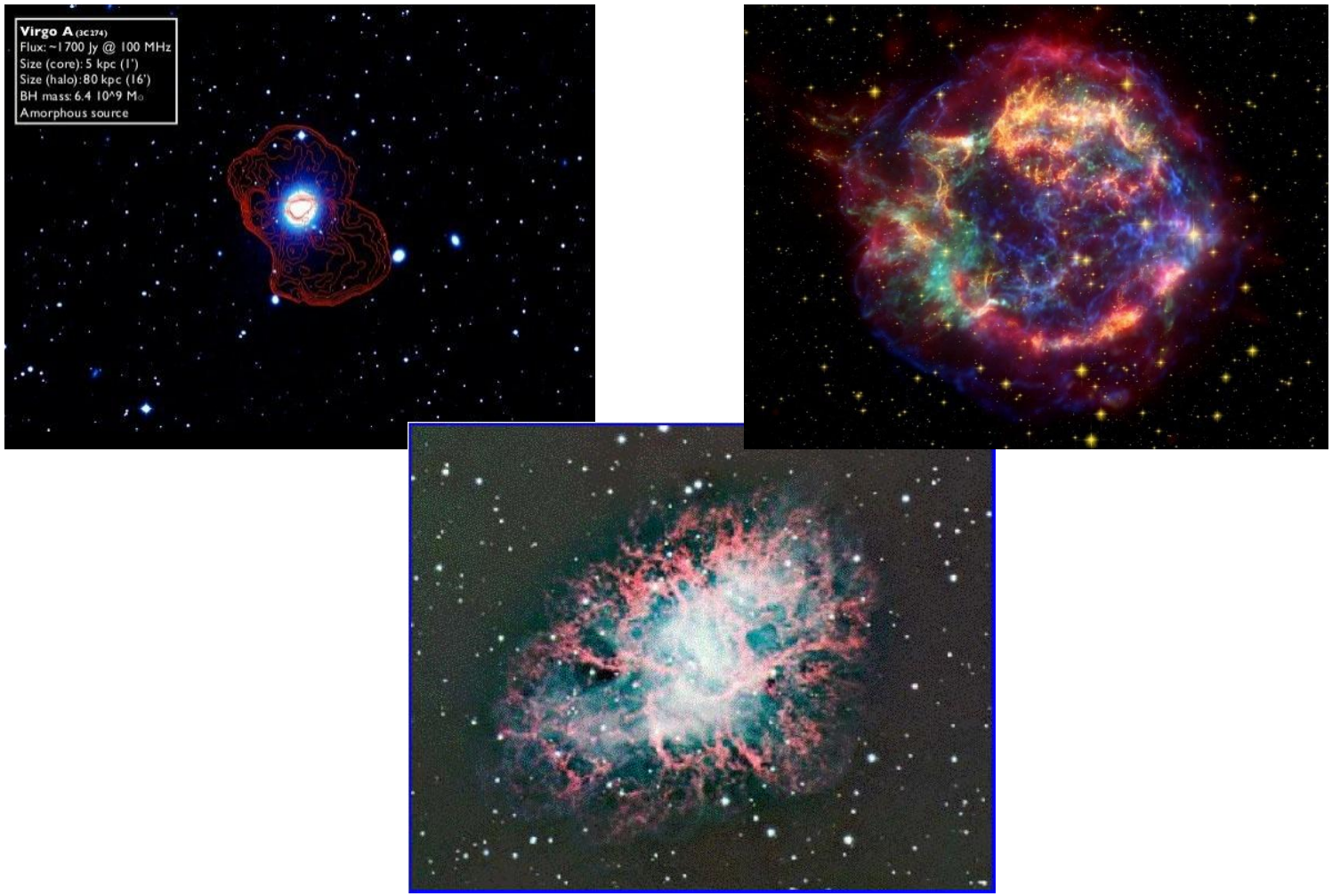

Fig.11.

Break frequencies (left) and exponent of scintillation spectra (right) which were measured during the observations

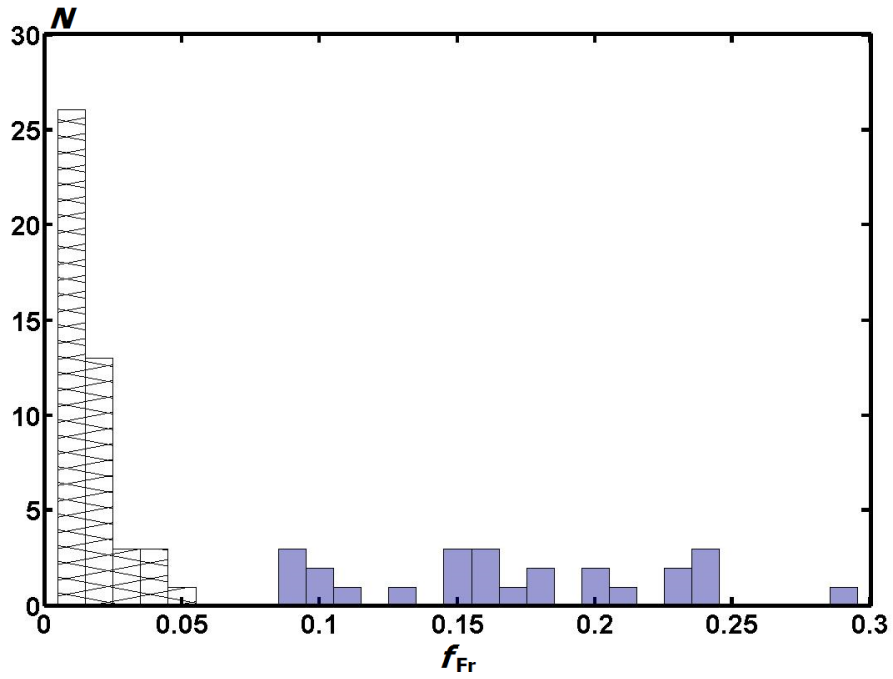

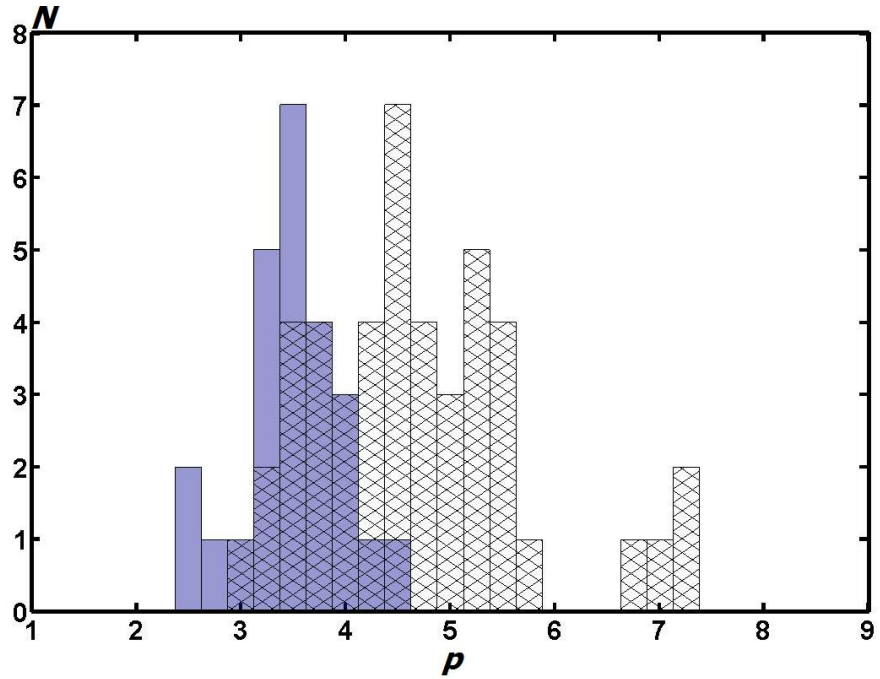

Fig. 12. Shaded histograms correspond to ionospheric scintillations and blue histograms are interplanetary ones.

Coefficients of frequency (left) and spatial (right) correlation which were measured during the observations

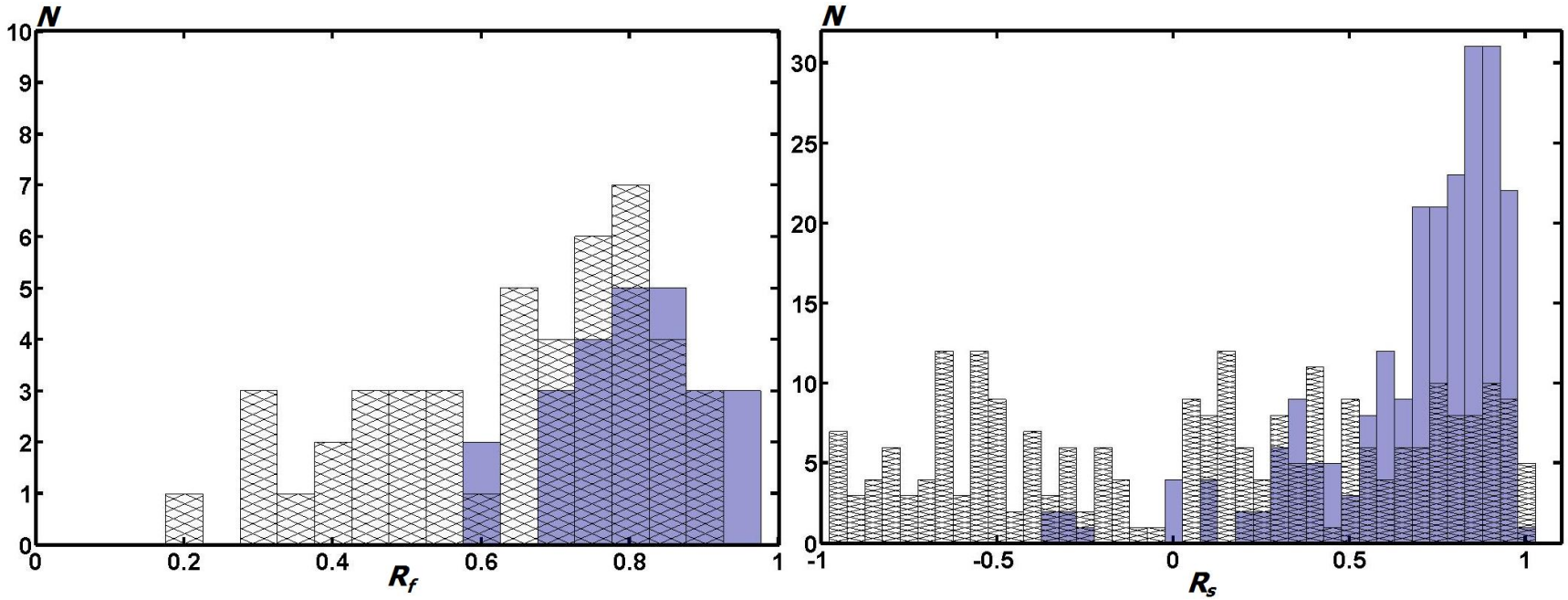

Fig. 13. Shaded histograms correspond to ionospheric scintillations and blue histograms are interplanetary ones.

Scintillation index which was measured during observations

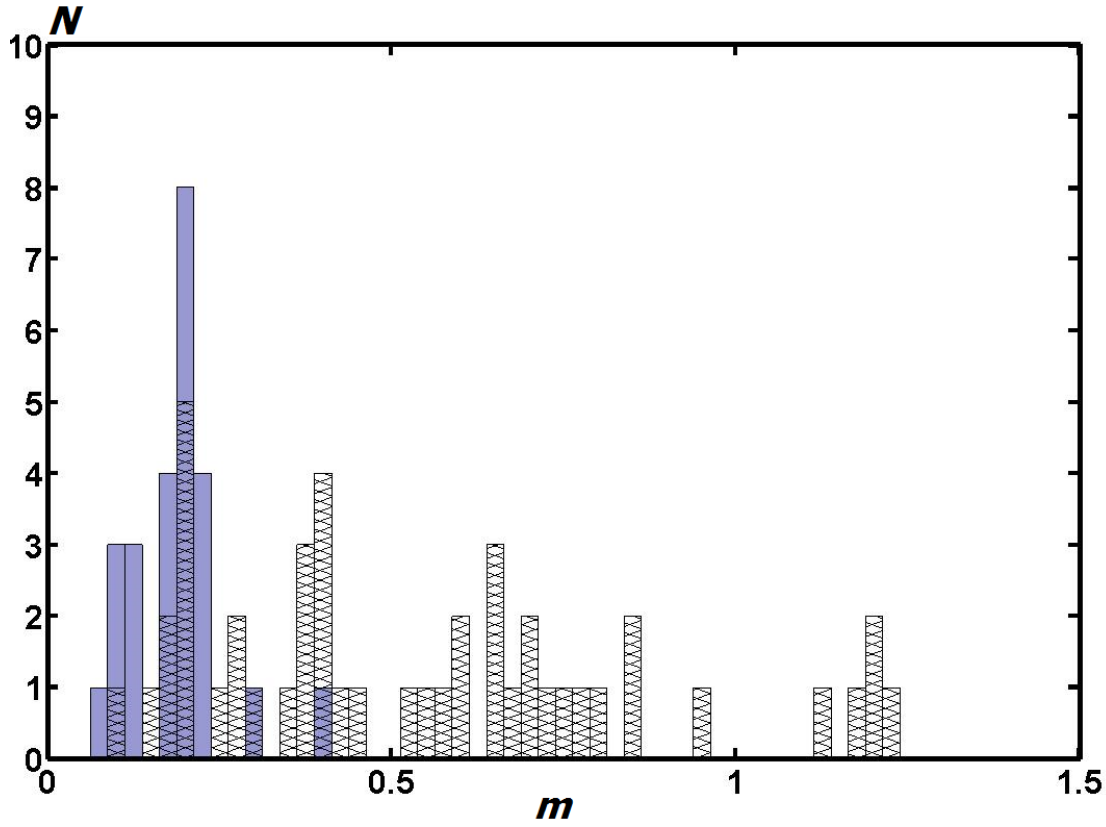

Fig. 14. Shaded histogram corresponds to ionospheric scintillations and blue histogram is interplanetary ones

Scintillation index versus spatial correlation coefficient

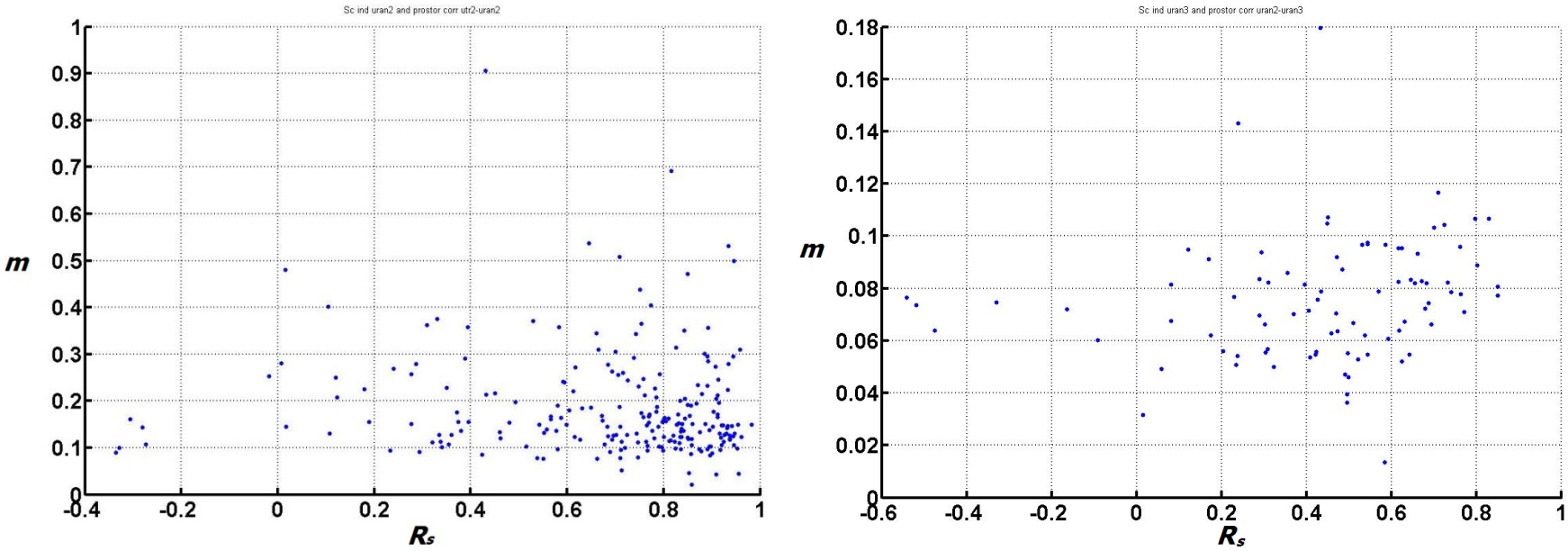

Fig. 15. URAN-2 scintillation index versus spatial correlation coefficient UTR-2 – URAN-2 (left). URAN-3 scintillation index versus spatial correlation coefficient URAN-2 – URAN-3 (right).

Scintillation index versus spatial correlation coefficient

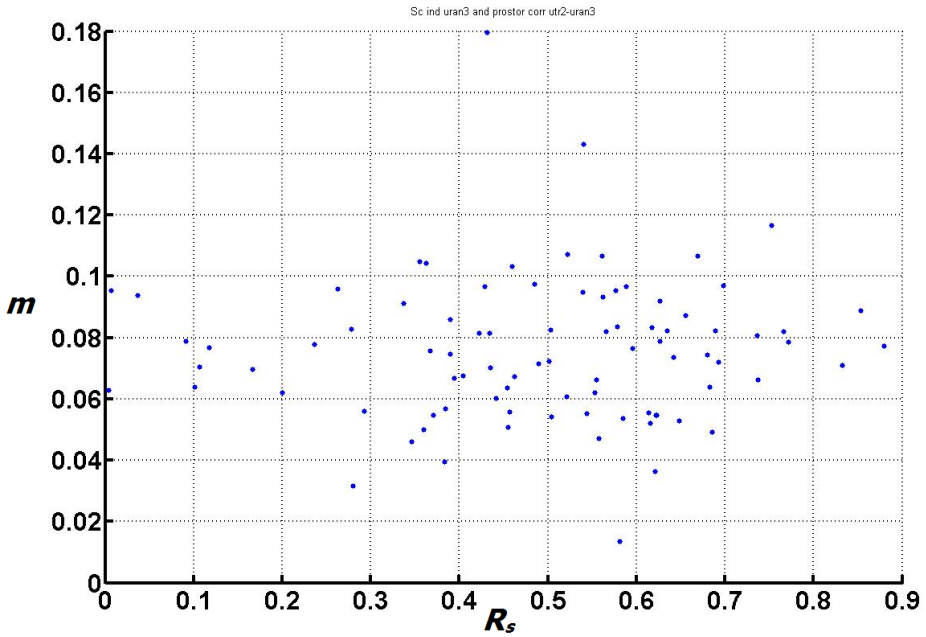

Fig. 16. URAN-3 scintillation index versus spatial correlation coefficient UTR-2 – URAN-3

Conclusions

Obtained results can be used for:

1. improving techniques used for estimation of the interplanetary and ionospheric plasma parameters;
2. separation interplanetary and ionospheric scintillations;
3. estimation of the interfering influence of the interplanetary and ionospheric plasma during radio astronomy experiments of a wide range of targets;
4. analysis of the interplanetary scintillations at other frequencies.